ELSEVIER

Journal of Pharmaceutical and Biomedical Analysis
14 (1995) 155–164

JOURNAL OF
PHARMACEUTICAL
AND BIOMEDICAL
ANALYSIS

Determination of the pharmaceutical peptide TP9201 by post-column reaction with copper(II) followed by electrochemical detection ☆

Steven J. Woltman [a], Jian-Ge Chen [a], Stephen G. Weber [a,*], James O. Tolley [b]

[a] *Box 109, Chevron Science Center, University of Pittsburgh, Pittsburgh, PA 15260, USA*
[b] *Telios Pharmaceuticals, Inc., 4757 Nexus Center Drive, San Diego, CA 92121, USA*

Received for review 29 May 1995; revised manuscript received 18 July 1995

Abstract

An electrochemical detection method was applied to the determination of the synthetic peptide TP9201 (Telios Pharmaceuticals). The method utilizes reversed-phase HPLC, followed by post-column formation of Cu(II)–peptide complexes to render peptides electrochemically active via the Cu(III/II) couple. TP9201 is cyclic and *N*-amidated; the lack of a free amine precludes the use of typical fluorescent labeling reagents. Neither the cyclic structure nor the *N*-amidation prevented the copper complexation reaction, however. The detection limit in bovine serum was 20 nM, limited by interfering sample peaks, and the detector response was linear in a range 10–400 nM.

Keywords: Peptide; TP9201; Reversed-phase high performance liquid chromatography; Electrochemical detection; Copper; Biuret

1. Introduction

The biological activity of peptides containing the Arg-Gly-Asp (RGD) integrin binding sequence has been a subject of much recent study. The pharmaceutical compound TP9201 (Telios Pharmaceuticals) is a synthetic RGD-containing peptide that selectively inhibits the binding of fibrinogen to the integrin (cell adhesion receptor $\alpha_{IIb}\beta_3$) on platelets, modulating thrombus formation while not prolonging bleeding time [1]. There is a need to determine blood levels of TP9201 for clinical trials with a detection limit of 10–20 nM.

Peptides are typically determined by HPLC or immunoassay. In the case of HPLC, detection is generally based upon either UV absorbance of the peptide bond (~215 nm) or precolumn reaction with amine-reactive fluorogenic labels, e.g. *o*-phthalaldehyde (OPA), followed by post-column fluorescence detection. A method for the determination of TP9201 based upon HPLC separation followed by UV detection (215 nm) has been published [2]; the limit of quantitation was in the

☆ Presented at the Sixth International Symposium on Pharmaceutical and Biomedical Analysis, April 1995, St. Louis, MO, USA.

* Corresponding author.

SSDI 0731-7085(95)01623-6

micromolar range. The method used a trichloroacetic acid (TCA) precipitation procedure that diluted the sample fourfold. The method was subsequently improved by adoption of acetonitrile precipitation, fivefold preconcentration and use of a 200 nm wavelength to improve sensitivity (J. Tolley, unpublished data); this affords a detection limit of approximately 50 ng ml^{-1} (~44 nM). This is the HPLC method currently in use.

Achieving further improvements in the detection limit of TP9201 presents an interesting analytical challenge. TP9201 is a cyclic, cystine-bridged nonapeptide (Fig. 1). The amine terminus is acetylated, precluding the use of amine-reactive fluorescent labels. The electrochemical activity of peptides containing typtophan or tyrosine residues has been utilized for post-column electrochemical detection [3,4]. However, the single tyrosine residue present in TP9201 is methylated; therefore, aside from the disulfide bond, the peptide contains no electroactive functional groups. Electrochemical detection of disulfides using a dual mercury/gold amalgam electrode was described by Allison and Shoup [5]. The detection limit (signal-to-noise ratio = 3) for oxidized glutathione standards in water was 0.3 μM, two orders of magnitude above the desired detection limit.

A post-column electrochemical detection method exists for peptides [6–10]. The method does not require that a free amine be present, or that any intrinsic electrochemical activity exist in the peptide. The method is compatible with gradient elution. It is based upon the following phenomena: (1) peptides react with copper(II) in alkaline solution [11–13] to form tetradentate copper(II) complexes (the biuret reaction), as illustrated in Fig. 2; and (2) the peptide complexation of copper(II) stabilizes the copper(III) oxidation state [11,12], permitting anodic oxidation of Cu(II) to Cu(III) at modest potentials in aqueous solution. In addition, the Cu(III) survives long enough to be detected by cathodic reduction to Cu(II) at a second downstream electrode.

The above properties of copper–peptide complexes provide the basis for a reactive labeling scheme that is specific for the characteristic repeating structure of the peptide backbone. The scheme is embodied as follows: (1) reactive labeling of eluting peptides is performed via post-column addition of alkaline copper tartrate reagent ("biuret reagent") upstream of a heated post-column reactor; and (2) the resulting Cu(II)–peptide complexes are detected electrochemically via the reversible Cu(III/II) couple. A thin-layer electrochemical detector is used in an upstream anode/downstream cathode configuration.

The upstream anode generates Cu(III)–peptide complexes and the downstream cathode reduces Cu(III)–peptide to Cu(II)–peptide. Both the anode and cathode typically give usable signals; however, the cathode signal generally exhibits better selectivity and signal-to-noise ratio.

From previous work, it is known that *N*-acylated peptides such as TP9201 react more slowly with copper(II) than similar peptides having a free amine group [14]. It is also known that the resulting complexes have a low oxidation potential compared with most peptide complexes [11,14]. The reaction rates of peptides with copper can be determined by means of UV–Vis absorbance measurements; the copper peptide complexes ab-

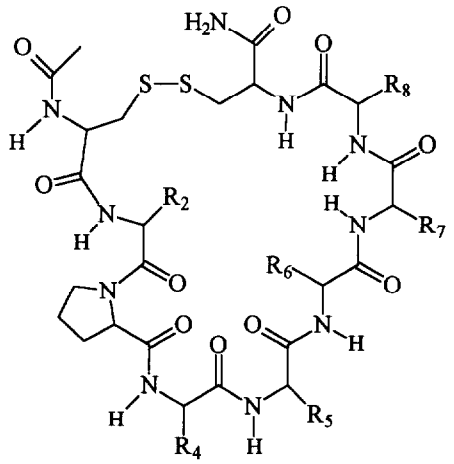

TP9201

CNPRGD(Y-OMe)RC

Fig. 1. Structure of TP9201.

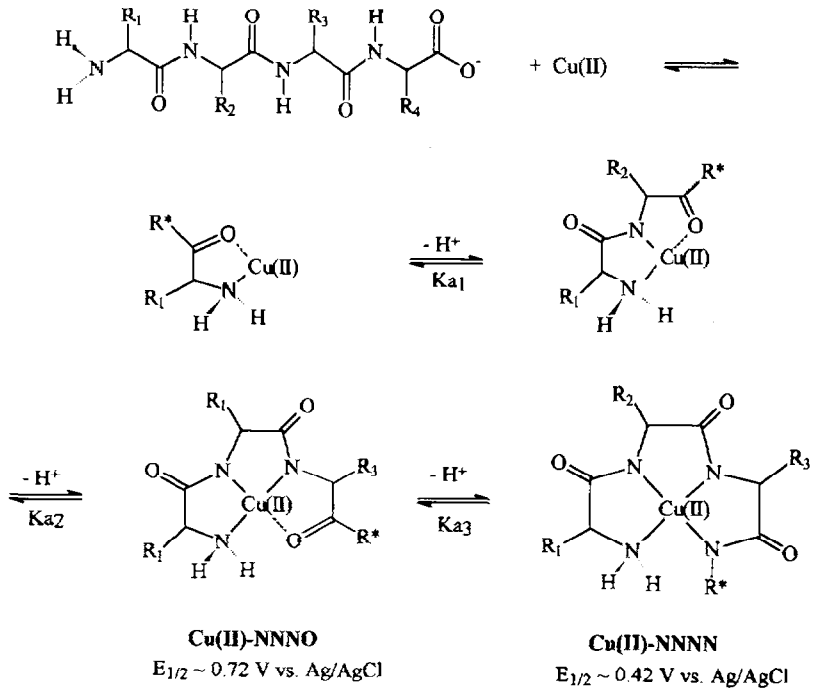

Fig. 2. Generic scheme for formation of copper(II)–peptide complex by successive deprotonation of amide nitrogens. R* indicates that portion of the peptide not immediately complexed to the copper. The peptide shown has a free primary amine, which is not the case with TP9201; the exact structure of the TP9201 complex is unknown.

sorb in the visible region of the spectrum, and indeed the biuret reaction has been widely used as the basis of a colorimetric assay for total protein [15]. The electrochemistry of the resulting complexes can be studied most easily by means of the rotating ring–disk electrode [16]. This instrument provides hydrodynamic voltammograms much more rapidly than does flow injection analysis.

Development work to date has been largely concerned with characterization of the complexation kinetics and electrochemical behavior of generic classes of peptides. Determination of TP9201 in serum affords an opportunity to apply the method to a peptide analyte in a typical biological sample matrix. In addition, the cyclic structure of the peptide is interesting, as representative of a class of cyclic peptide structures.

2. Experimental

2.1. Reagents

All solid reagents were of ACS grade. Sources were as follows: copper sulfate pentahydrate, 50 wt.% sodium hydroxide, and sodium hydrogen carbonate, Fisher Scientific (Pittsburgh, PA, USA); disodium tartrate dihydrate, Baker (Phillipsburg, NJ, USA); sodium carbonate and HPLC-grade acetonitrile, EM Science (Gibbstown, NJ, USA); trifluoroacetic acid and HPLC-grade 1-propanol, Aldrich (Milwaukee, WI, USA); and boric acid, Mallinckrodt (Paris, KY, USA). The copper sulfate pentahydrate and disodium tartrate dihydrate were recrystallized once from water; all other reagents were used without further purification. Doubly deionized water from a MilliQ system (Millipore, Bedford, MA, USA) was

used for all solutions. TP9201 was manufactured by Telios Pharmaceuticals (San Diego, CA, USA).

2.2. Kinetics of complex formation by visible spectrophotometry

Kinetic studies employed an IBM 9420 UV–Vis spectrophotometer with a thermostated 1 cm borosilicate cuvette. Biuret reagent (copper sulfate–disodium tartrate–borate, adjusted to pH 10.0 with NaOH) was mixed rapidly in situ with TP9201 to give final concentrations of 0.25 mM TP9201, 10 mM Cu^{2+}, 30 mM tartrate and 0.2 M borate. Both components of the mixture were equilibrated at the reaction temperature before mixing. The absorbance maximum of the complex (523 nm) was established by heating a batch of the reaction mixture at 50 °C for until further development of the visible spectrum ceased, and determining the zero crossing of the first derivative of the final spectrum. Kinetic measurements were performed by monitoring the absorbance of newly mixed solutions at the absorbance maximum, first at 10 s after mixing and then at 30 s intervals thereafter.

2.3. Rotating ring–disk electrode hydrodynamic voltammetry

The rotating ring–disk apparatus consisted of a DT-29 glassy carbon/glassy carbon ring–disk electrode, ASR-2 analytical rotator and RDE-3 potentiostat (all from Pine Instrument, Grove City, PA, USA). A platinum grid auxiliary electrode and BAS Ag/AgCl reference electrode were used. All potentials were reported relative to this reference. Before each run, the electrode was wet-polished with 0.05 μm alumina. The disk (anode, generator) and ring (cathode, collector) signals were filtered with a Wave-Tek Model 852 filter (San Diego, CA, USA) set for low pass with an 11 Hz cut-off frequency.

TP9201 was mixed with excess copper sulfate–disodium tartrate mixture. This was dissolved in aqueous carbonate buffer (carbonate–hydrogen carbonate) (pH 10.0) to final concentrations of 0.100 mM TP9201, 0.5 mM copper sulfate, 1.5 mM tartrate and 0.2 M carbonate. The mixture was heated at 50 °C for 5 min to drive the complexation reaction, then cooled to room temperature. A temperature of 25 °C was used for subsequent voltammetry.

Voltammetry was performed by first initiating RRDE rotation, then sweeping the disk potential from 0.00 to 0.90 V vs. Ag/AgCl at 0.60 V min^{-1}. The ring was maintained at a constant potential of 0.00 V. A series of rotation speeds from 150 to 10 000 rpm were used; 150 rpm approximately corresponds to the hydrodynamic time-scale of the thin-layer electrochemical detector as used for TP9201 determinations (0.35 ml min^{-1} total flow rate, 16 μm spacer). A copper–tartrate blank voltammogram was subtracted from the TP9201 voltammogram. Data were collected using EZChrom chromatography software (Scientific Software, San Ramon, CA, USA) in conjunction with a DT2802 interface board (Data Translation) running on a DTK personal computer. Half-wave potentials were identified using the potentials at which the second derivative of the voltammograms crossed zero.

2.4. HPLC–ED determination of TP9201

A Waters 600 MS pump (Bedford, MA, USA) was used for all HPLC runs. Three different columns were tested for TP9201 chromatography: a Vydac C_4 protein column, 5 μm, 300 Å, 250 × 4.6 mm i.d. (Alltech); a Delta-Pak C_{18}, 5 μm, 300 Å, 150 × 2 mm i.d. (Waters); and a Hypersil C_{18}, 3 μm, 120 Å, 100 × 1 mm i.d. (Keystone Scientific, Bellefonte, PA, USA). Mobile phase flow rates were 1.00, 0.25 and 0.050 ml min^{-1} and post-column reagent flow rates were 0.40, 0.10 and 0.02 ml min^{-1}, respectively. The post-column reactor in each case gave a residence time of approximately 1 min at 50 °C. The 2 mm i.d. Delta-Pak column gave the best combination of sensitivity and separation efficiency and was employed for all analytical work; the experimental conditions described below pertain to this column.

A Waters Bondapak C_{18} guard column was installed upstream of the analytical column. Elution was via an acetonitrile gradient. Solvent A was aqueous trifluoroacetic acid (0.1%, v/v)–1-propanol (3.0%, v/v) and solvent B was trifluoroacetic acid (0.1%, v/v)–1-propanol (3.0%,

v/v)–acetonitrile (60%, v/v)–in water. The gradient progressed from 0 to 50% phase B in 30 min. The injection volume was 100 μl. An Isco Model 100 DM syringe pump (Lincoln, NB, USA) was used to pump the post-column reagent into a mixing Y downstream of the column. The post-column reagent consisted of 0.5 mM copper sulfate, 3.0 mM disodium tartrate and 1.2 M carbonate buffer (pH 9.9; pH when diluted in mobile phase, 10.1).

The post-column reactor consisted of knitted 0.01 in. Teflon tubing of a sufficient length to give a residence time of 1.1 min. Both the column and reactor were enclosed in a BAS LC-23A column heater maintained at 50 °C. Electrochemical detection employed a BAS CC-5 thin-cell detector with dual glassy carbon electrodes; the potential was controlled by dual BAS LC-4C potentiostats. The post-column reagent stream was directed through the cell preheater module of the CC-5, set at 50 °C, and then to the mixing Y upstream of the reactor. The upstream electrode (anode) was maintained at 410 mV and the downstream electrode (cathode) at 85 mV vs. Ag/AgCl; sensitivities were set at 50 and 5 nA V^{-1}, respectively. The Teflon spacer used to gasket the thin cell was of 0.0005 in. (16 μm) thickness.

Data were collected using EZchrom chromatography software. Peaks were assigned with the Manual Peak utility of the program.

Following preliminary experimentation establishing feasibility, retention time, etc., the analyses of both standards and spiked serum samples were performed on four different days over a period of approximately 1 week.

2.5. Calibration standards

Concentrated TP9201 stock solutions were diluted in doubly deionized water and frozen at −20 °C. The standards were thawed immediately before HPLC injection and refrozen immediately afterwards.

2.6. Spiked serum samples

Bovine serum (Sigma S-7140, shipped frozen) was thawed, divided into 3.00 ml aliquots in 15 ml polypropylene conical centrifuge tubes (Corning 25319-15) and promptly refrozen. The aliquots were thawed for 10–20 min before spiking. Concentrated TP9201 stock solutions (30.0 μl) were spiked into the thawed bovine serum aliquots to give final concentrations of 10, 20, 50, 100 and 200 nM. Low-speed vortexing was used to mix the samples. The samples were then promptly (within 5–10 min) subjected to the following acetonitrile precipitation–preconcentration procedure, adapted from that used with the current UV detection-based HPLC method.

To precipitate large serum proteins, 6.00 ml of ice-cold acetonitrile was added to each tube. The tubes were vortex mixed and inverted vigorously, then put on ice for 10 min. The samples were then maintained at 4 °C throughout subsequent centrifugation steps. After centrifugation at 2050*g* for 20 min, the entire supernatant liquid was poured into clean 15 ml tubes and centrifuged at 2050*g* for 2 h; the long centrifugation time was necessitated by the low-speed centrifuge available. The top 6.00 ml of supernatant liquid was pipetted into clean 15 ml tubes; these were placed in a 50 °C water-bath and blown dry under streams of argon directed through hypodermic needles. The dried residue was reconstituted in 1000 μl of deionized water and centrifuged in a 0.2 μm nylon membrane device (Rainin 7016-021) at 2050*g* until most (~90%) of the liquid had penetrated the membrane. The filtrates were frozen at −20 °C and thawed immediately before HPLC analysis. The procedure provides a twofold volume preconcentration.

3. Results and discussion

3.1. Kinetics of complex formation by visible spectrophotometry

Copper(II)–peptide complexes exhibit colors ranging from blue to red. The broad absorbance bands, spanning the visible spectrum, result from d–d electronic transitions. The value of λ_{max} is determined by the identity of the donor ligands. A widely used empirical correlation by Billo [13] describes this relationship quantitatively, subject to certain constraints: that the complex be strictly

square planar, that axial water molecules be present and that donor groups be present in the axial positions if water is not. Also, the effect of ring strain is neglected. The Cu(II)–TP9201 complex is believed to meet these requirements. The correlation predicts λ_{max} values of 515 (±15) nm for complexation of copper(II) by four deprotonated amide (amido) nitrogens and 569 (±15) nm for complexation of copper(II) by three amino nitrogens and one carbonyl oxygen.

The measured value of λ_{max}, 523 n, is consistent with Cu(II) complexed by four amido nitrogens, and possibly a lesser portion having Cu(II) complexed by three amido nitrogens and one carbonyl oxygen.

The expected increase in reaction rate with temperature is apparent from plots of the development of absorbance with time (Fig. 3). It is interesting that the final absorbance values also increase with temperature, with the final molar absorptivity ranging from 104 l mol^{-1} cm^{-1} at 25 °C to 232 l mol^{-1} cm^{-1} at 45 °C. It is possible that the structure of the complex depends on the temperature. Values for the first-order rate constant k can be obtained from the relationship $A = A_0(1 - e^{-kt})$, where A is absorbance at a particular time and A_0 is the absorbance at 100% reaction; k is obtained as the slope of a plot of $\ln(1 - A/A_0)$ versus time. The values obtained are listed in Table 1. The absorbance maximum, molar absorptivities and rate constants are very close to those measured for other *N*-amidated peptides [14].

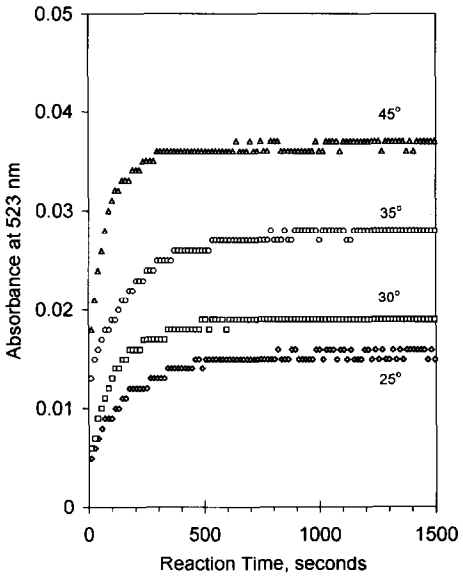

Fig. 3. Development of the absorbance spectrum of the copper(II)–TP9201 complex at different temperatures.

Table 1
Pseudo-first-order rate constant and half-time for formation of the copper(II)–TP9201 complex at different temperatures

Temperature (°C)	$k \pm$ S.E. (s^{-1})	$t_{1/2} \pm$ S.E. (s)
25	0.0043 ± 0.0002	161 ± 8
35	0.0050 ± 0.0001	139 ± 3
30	0.0078 ± 0.0003	89 ± 3
45	0.0090 ± 0.0004	77 ± 3

The kinetic data indicate that the reaction should be approximately 50% complete in the 1.1 min residence time of the 50 °C reactor. This is consistent with the electrochemical sensitivity found for the electrochemical detector (see below).

3.2. Rotating ring–disk electrode analysis

Two waves were observed in the hydrodynamic voltammograms (Fig. 4); these were visible in the signals from both the anode (disk, generator) and cathode (ring, collector) electrodes. The first wave had a half-wave potential of 0.35 V vs. Ag/AgCl and the second wave a half-wave potential of 0.70 V. The relative heights of the cathodic waves were dependent on rotation speed, with the first wave ranging from 60% of the total signal at 10 000 rpm to 80% at 150 rpm. By equating mass transport rates calculated from theory [17,18] it can be determined that 150 rpm approximately corresponds to the hydrodynamic time-scale of the electrochemical detector as used with the 2 mm i.d. Delta-Pak column. In contrast to the cathode, the relative heights of the two anodic waves do not change significantly with rotation speed, indicating that the change in the relative cathodic wave heights is due to instability of the Cu(III) form produced at the higher potential. It is apparent in Fig. 4 that the second wave is a relatively larger portion of the total signal at the

disk than at the ring; the Cu(III)–peptide complex produced at the potential of the second wave decays in transit from the disk to the ring. The potentials of the two waves are consistent with copper(II) complexed by four amido nitrogens (first wave) and copper(II) complexed by three amido nitrogens and one carbonyl oxygen (second wave) [11].

It is known that thiol is capable of acting as a donor atom in copper(II) complexes of sulfur-containing peptides, e.g. synthetic *N*-mercaptoacetyl peptides [19], and that dithalooxalato-*S,S'* complexes of copper [20] are capable of stabilizing the copper(III) oxidation state. On the other hand, examples of disulfide-bridged cyclic peptide complexes of copper(II) are known in which the disulfide bond is intact [21,22]. Also, the spectroscopic and electrochemical data are consistent with complexation by amido nitrogens and by amido nitrogens plus carbonyl oxygen. The presence of a form of the Cu(II)–TP9201 complex

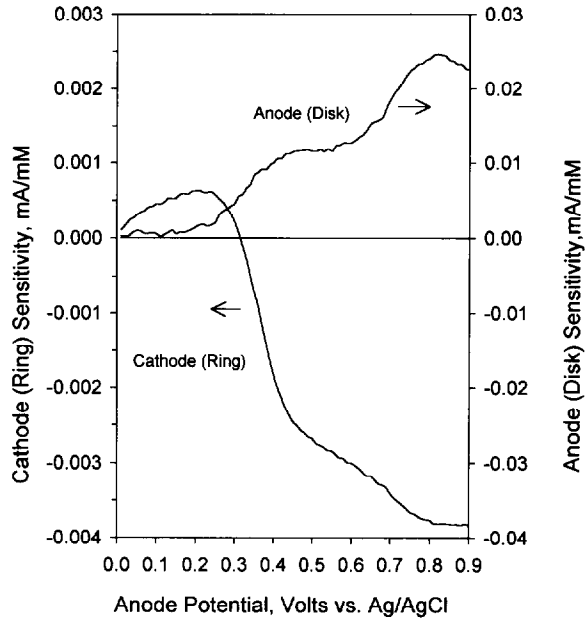

Fig. 4. Rotating ring–disk electrode voltammogram of TP9201; rotation speed = 150 rpm. The ring electrode is maintained at a constant potential and serves as a collector for the copper(III) species generated as the potential is swept at the disk (anode). The cathodic current is here depicted as negative; the positive excursion of the cathodic current early in the run is an artifact of the background subtraction.

having sulfur as a donor atom is therefore considered unlikely.

For advantages of selectivity and signal-to-noise ratio, the use of the signal from the first wave was an obvious choice. For HPLC detection, an anode (generator) electrode potential (0.41 V) in the plateau region of the first wave was chosen based upon the RRDE results.

3.3. HPLC–ED determination of TP9201

As mentioned in the Experimental section, 150 × 2 mm i.d. Delta-Pak C_{18} was selected from the available columns as the best compromise between sensitivity and separation performance. The sensitivity advantage obtained by using smaller columns is illustrated by the values listed in Table 2. In general, smaller columns will give lower detection limits because of decreased sample dilution and increased electrolysis [23]. Unfortunately, the 1 mm i.d. column gave TP9201 peaks with severe tailing; note the asymmetry factor of 3.8. Other peptide standards gave asymmetry factors of 1.2–1.7 on this column, indicating that reactor dead volume, etc., was not the source of the problem. It was suspected that the pore size or structure of the Hypersil C_{18} material used in the 1 mm i.d. column might slow the rate of interphase mass transport, resulting in the peak tailing. The 4.6 mm i.d. Vydac C_4 column, with a larger 300 Å pore size, gave symmetrical peaks. The 2 mm i.d. Delta-Pak C_{18} column, with a 300 Å pore size, also produced symmetrical peaks, with a sensitivity improvement over the larger 4.6 mm i.d. column.

According to theory [17], peak area (coulombs per mole) should scale with the $-2/3$ power of both the volumetric flow rate, U, and the spacer thickness, b. The increase in sensitivity from the largest to smallest column, although substantial, is less than predicted by theory. This is due at least in part to the use of a lower pH post-column reagent for the smaller columns than for the largest column. There remains a deficiency in sensitivity not accounted for by this consideration, however. The 1 mm i.d. column, for example, despite peak tailing, should exhibit a 17-fold improvement in peak area over the 4.6 mm i.d.

Table 2
Performance of standard-, narrow- and micro-bore columns in chromatography of TP9201 standards

Parameter	Stationary phase		
	Vydac C_4	Delta-Pak C_{18}	Hypersil C_{18}
Length × i.d. (mm)	4.6 × 250	2 × 150	1 × 100
Particle diameter (μm)	5	5	3
Pore size (Å)	300	300	120
pH of post-column reagent[a]	10.2	10.1	10.0
Spacer thickness (μm)	51	16	16
Flow rate in cell (ml min^{-1})	1.40	0.35	0.070
Fluid velocity in cell (cm s^{-1})	6.1	6.1	1.2
Asymmetry	1.4	1.5	3.8
Peak area (nC $pmol^{-1}$)	0.57	1.2	3.1
Peak height (nA $nmol^{-1}$)	16	31	51

[a] After mixing with mobile phase.

column; the actual improvement is approximately fivefold. This may represent an opportunity for a further improvement in detection limit.

Typical chromatograms of TP9201 are shown in Fig. 5. The TP9201 peaks were well separated from large interference peaks. The retention time, however, was 16.3 min for standards in water and 15.8 min for samples in serum, possibly because of modification of the column by the components of the sample. The reproducibility of the TP9201 retention time was poorer in serum, with a standard deviation of 0.17 min compared with 0.04 min for the standards. A small interference peak co-eluted with the analyte peak, limiting detectability to 10 nM. Outside of the region where TP9201 eluted, the peaks observed in the serum samples were not completely consistent from sample to sample, e.g. the large peak at ~27 min in the 200 nM sample and that at ~18 min in the 10 and 20 nM samples. The source of this variation is unknown, but may be due to variability in the filtration or drying steps. Hydrolysis of serum peptides is another possible source of these peaks; however, the serum aliquots all came from the same batch, and precipitation with acetonitrile was completed within 20–30 min of thawing the frozen aliquots, minimizing the time during which proteolytic enzymes could operate in the individual serum samples.

The preconcentration used with the serum samples (twofold) could be increased by reconstituting the dried samples in a smaller volume of deionized water. It was found, however, that problems with retention time reproducibility increased when fivefold perconcentration was attempted, and so the twofold procedure was used. A greater degree of preconcentration may be possible with a different reversed-phase column, e.g. C_4-bonded silica.

The relatively noisy anode signal was not used for quantitation of the analyte, and these chromatograms are not shown. However, it is instructive that the anodic mass sensitivity, 3 nC $pmol^{-1}$, was approximately 40% that of a well behaved standard peptide (e.g. Gly-Gly-Phe-Leu) that reacts completely and exhibits a single voltammetric wave under the conditions used. This is consistent with the approximately 50% reaction extent predicted from the spectroscopic kinetic study and the observation that the first wave was 80% of the total signal in the RRDE voltammogram (50% × 80% = 40%). The theoretical collection efficiency of the thin detector cell was 40%, i.e. that fraction of material generated at the upstream anode encountered the downstream electrode. The cathode and anode signals had the expected ratio.

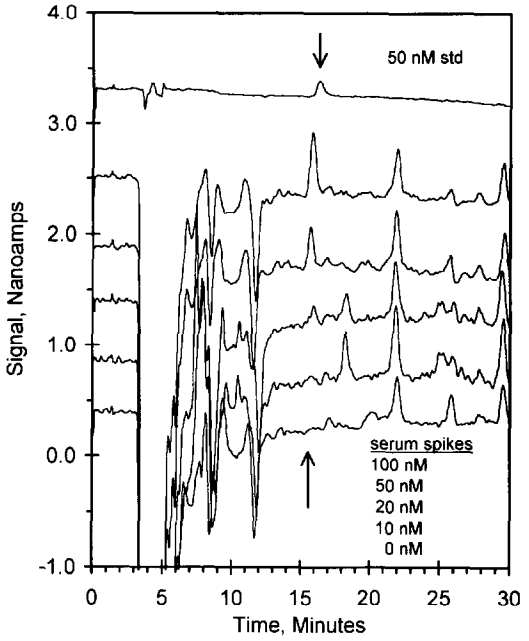

Fig. 5. Representative chromatograms: 50 mM TP9201 standard in water and various concentrations in serum. The concentrations listed for the serum spikes are the original concentrations; a twofold volume preconcentration in the sample preparation has nominally doubled the listed concentrations.

Determinations of TP9201 standards in deionized water and for TP9201 spiked in serum were found to be linear with respect to both peak height and peak area (Tables 3 and 4). The nominal concentratoins for TP9201 in serum were multiplied by two to account for the preconcentration. Peak area was a more reproducible measure of TP9201 in serum, but equivalent to peak height for standards in water. The detection limit in serum in the present study was 20 nM. The percentage recovery was estimated by dividing the slopes obtained for TP9201 in serum by the slopes obtained for TP9201 in water; the values obtained were 81 (±6)% for peak area and 89 (±13)% for peak height. The stated uncertainties are 95% confidence intervals. TP9201 is known to hydrolyze in plasma; the high recovery indicates that relatively little material was hydrolyzed in the short time before acetonitrile precipitation.

As mentioned in the Introduction, the current UV detection-based HPLC method attains a detection limit of approximately 44 nM, using fivefold preconcentration. The 20 nM detection limit of the electrochemical method, obtained using only a twofold preconcentration, thus affords a significant improvement over the current UV detection method. Difficulties encountered in the present study with the chromatography of serum samples (change in retention time, peak tailing) are not specific to electrochemical detection, and should be amenable to improvement via suitable changes in methodology.

4. Conclusion

Although one should be cautious in generalizing from bovine serum to other matrices, e.g. human blood samples, it appears feasible to determine TP9201 at concentrations well below 50 nM in biological samples, with a detection limit of 20 nM in the particular samples used in this investigation. It should be straightforward to apply the methodology to other synthetic and natural peptides in real samples.

It was found in that good separations of TP9201 require attention to the stationary phase

Table 3
Calibration graph regressions

Regression variable	Peak area		Peak height	
	Anode	Cathode	Anode	Cathode
Slope ± S.E.	3.17 ± 0.27 nC pmol^{-1}	1.29 ± 0.030 nC pmol^{-1}	0.00960 ± 0.00059 nA nM^{-1}	0.003259 ± 0.000059 nA nM^{-1}
Intercept ± S.E.	1.21 ± 2.72 nC	−0.981 ± 0.439 nC	0.04141 ± 0.00598 nA	−0.00075 ± 0.00087 nA
r^2	0.933	0.994	0.964	0.996
n	12	13	12	13

Table 4
Sensitivity of TP9201 spiked in serum

Regression variable	By peak area		By peak height	
	Anode	Cathode	Anode	Cathode
Slope ± S.E.	3.27 ± 0.57 nC pmol^{-1}	1.050 ± 0.032 nC pmol^{-1}	0.00973 ± 0.00012 nA nM^{-1}	0.00291 ± 0.00018 nA nM^{-1}
Intercept ± S.E.	-6.6 ± 13.0 nC	-0.14 ± 0.66 nC	0.00877 ± 0.0274 nA	0.0413 ± 0.037 nA
r^2	0.943	0.994	0.971	0.973
n	4	11	4	11

material; the morphology of the large-pore (300 Å) Vydac and Delta-Pak material appears to be superior to that of Hypersil for this purpose. Microbore reversed-phase columns with the somewhat fragile 300 Å material have recently become available. The use of microbore columns decreases sample dilution and enhances electrolysis efficiency in electrochemical cells due to the flow rate [23]. Use of a 1 mm i.d. column with suitable stationary phase material should therefore result in a substantial increase in sensitivity over the 2 mm i.d. column used in the present study.

Acknowledgment

We thank the NIH for financial support through Grant GM-44842.

References

[1] S. Cheng, W.S. Craig, D. Mullen, J.F. Tschopp, D. Dixon and M.D. Pierschbacher, J. Med. Chem., 37 (1994) 1–8.
[2] J.F. Tschopp, W.S. Craig, J. Tolley, J. Blevitt, C. Mazur and M.D. Pierschbacher, Methods Enzymol., 245 (1994) 556–569.
[3] J. Cummings, A. MacClellan, S.P. Langdon, E. Rozengurt and J.F. Smyth, J. Chromatogr. B, 653 (1994) 195–203.
[4] M.A. Kukucka and H.P. Misra, J. Chromatogr. B, 653 (1994) 139–145.
[5] L.A. Allison and R.E. Shoup, Anal. Chem., 55 (1983) 8–12.
[6] A.M. Warner and S.G. Weber, Anal. Chem., 61 (1989) 2664–2668.
[7] H. Tsai and S.G. Weber, J. Chromatogr., 515 (1990) 451–457.
[8] H. Tsai and S.G. Weber, J. Chromatogr. B, 542 (1991) 345–350.
[9] H. Tsai and S.G. Weber, Anal. Chem., 64 (1992) 2897–2903.
[10] J.G. Chen, S.J. Woltman and S.G. Weber, J. Chromatogr. A, 691 (1995) 301–315.
[11] F.P. Bossu, K.L. Chellapa and D.W. Margerum, J. Am. Chem. Soc., 99 (1977) 2195–2203.
[12] D.W. Margerum, Pure Appl. Chem., 55 (1983) 22–34.
[13] E.J. Billo, Inorg. Nucl. Chem. Lett., 10 (1974) 613–617.
[14] J.G. Chen, Doctoral Thesis, University of Pittsburgh, Chapter 6, in press.
[15] A.G. Gornall, C.J. Bardawill and M.M. David, J. Biol. Chem., 177 (1949) 751–766.
[16] S.J. Woltman, M.R. Alward and S.G. Weber, Anal. Chem., 67 (1995) 541–551.
[17] J.M. Elbicki, D.M. Morgan and S.G. Weber, Anal. Chem., 56 (1984) 978–985.
[18] W.J. Albery and M.L. Hitchman, Ring–Disc Electrodes, Clarendon Press, Oxford, 1971.
[19] Y. Sugiara, Inorg. Chem., 17 (1977) 2176–2182.
[20] T.I. Imamura, M. Ryan, G. Gordon and D. Coucouvanis, J. Am. Chem. Soc., 106 (1984) 984–990.
[21] H. Kozlowski, B. Radomska, G. Kupryszewski, B. Lammak, C. Livera, L.D. Pettit and S. Pyburn, J. Chem. Soc., Dalton Trans., (1989) 173–177.
[22] W. Bal, H. Kozlowski, B. Lammek, L.D. Pettit and K. Rolka, J. Inorg. Biochem., 45 (1992) 211–219.
[23] E.J. Caliguiri and I.N. Mefford, Brain Res., 296 (1984) 159.